Low-temperature time-resolved photoluminescence characterization of 3,4,9,10-perylene tetracarboxylic dianhydride crystals

A. Yu. Kobitski,[1,2] R. Scholz,[1] I. Vragović,[1] H. P. Wagner,[3] and D. R. T. Zahn[1]
[1]*Institut für Physik, Technische Universität Chemnitz, D-09107 Chemnitz, Germany*
[2]*Department of Biophysics, University of Ulm, 89069 Ulm, Germany*
[3]*Department of Physics, University of Cincinnati, Cincinnati, Ohio 45221-0011*
(Received 18 February 2002; revised manuscript received 26 April 2002; published 29 October 2002)

In the present work, we investigate the recombination dynamics in α-PTCDA (perylene tetracarboxylic dianhydride) crystals with time-resolved photoluminescence (PL) techniques. From a data analysis based on three different recombination channels, we assign two decay times of $\tau_s=(33.5\pm2)$ ns and $\tau_m=(12.7\pm0.4)$ ns to radiative decay, while a faster component of $\tau_f=(3\pm1)$ ns is likely to have strong nonradiative contributions. Our findings are compared to recent investigations of the dispersion of Frenkel excitons and calculated radiative recombination rates for PL out of the minimum of the Frenkel exciton dispersion.

DOI: 10.1103/PhysRevB.66.153204 PACS number(s): 78.55.Kz, 78.20.Bh, 78.47.+p, 71.35.Aa

In recent years, molecular organic semiconductors were widely investigated because of their possible applications in organic light-emitting diodes and field-effect transistors. One of the most intensively studied molecules is 3,4,9,10,-perylene tetracarboxylic dianhydride (PTCDA). These planar molecules can form well ordered (poly)crystalline films on a variety of substrates.[1] Even though PTCDA films have been investigated for more than 10 years, the knowledge about absorption, relaxation, and recombination processes in PTCDA crystals and films is still rather limited. Recently it was demonstrated that the linear optical properties of polycrystalline PTCDA films[2] and the optical anisotropy of single crystals[3] can be analyzed with an approach based on the transfer of Frenkel excitons, including a realistic three-dimensional crystal structure with two molecules per unit cell.[4]

Low-temperature photoluminescence (PL) spectra have been investigated for amorphous PTCDA films deposited at low temperature,[5] heterostructures containing PTCDA layers,[1,6] and polycrystalline thin films deposited at different temperatures.[7] Further PL studies concentrated on a closely related compound, MePTCDI (N,N'-dimethylperylene 3,4,9,10,-bis-dicarboximide),[5,8] where the main PL bands characterizing the crystalline phase resemble the so-called *Y* band in PTCDA (Ref. 7) and the high-temperature PL of β-perylene.[9] Low-temperature time-resolved PL studies of PTCDA and MePTCDI revealed a strong dependence on layer thickness[1,6] and morphology,[5] where a decay rate of about 4 ns seems to be related to the monomer, while both slower[6] and faster[5] decays were observed, the latter probably being nonradiative in nature. Recent time-resolved PL spectra of MePTCDI within the first 100 ps after excitation were compared to a model including both Frenkel and charge-transfer excitons, revealing PL contributions far below the minimum of the calculated exciton dispersion.[10]

At higher temperatures the decay dynamics in polycrystalline films seem to be much faster,[8,11] except for a recent PL study of PTCDA at room temperature, revealing a decay time of about 9 ns.[12] However, for the time being, there seems to be no detailed study of time-resolved PL on single crystals of PTCDA in the 100-ns range, which will be the topic of the present work. Based on a careful numerical fitting procedure, we can extract three different contributions to the PL spectra with distinct decay rates. These findings are compared to recent calculations of the dispersion and Davydov splittings of Frenkel excitons in α-PTCDA.[4,13]

The α-PTCDA single crystals used in the present PL study were fabricated by double sublimation at 575 K under high vacuum (10^{-6} Pa). For the time-resolved PL measurements, the PTCDA crystal was excited with a pulsed dye laser synchronously pumped by a mode-locked Ar^+ ion laser, resulting in 20-ps pulses at an energy of 2.14 eV (580 nm). The intrinsic repetition rate of 80 MHz defined by the cavity length of the ion laser was reduced to 4 MHz using a cavity dumper. The diameter of the laser spot focused on the sample was about 250 μm, corresponding roughly to the smallest extension of the PTCDA needles. The time-resolved PL was analyzed using a CROMEX 250IS imaging spectrograph, and detected by a Hamamatsu C4334 Streakscope with a time resolution better than 50 ps. In order to protect the streakscope against stray light from the laser, a filter with a cutoff at 590 nm (2.10 eV) was used. In the range 1.5–2.1 eV investigated in the present work, the flatness of the spectral response of the entire measuring system was checked with black body radiation from a tungsten lamp with known emission spectrum, and therefore no spectral correction was applied to the subsequent PL measurements. For the low-temperature ($T=11$ K) measurements, a closed-cycle He cryostat CTI-Cryogenics was used.

The transient PL data were collected for 480 spectral sampling points in intervals of 0.585 nm and 480 time steps of 0.208 ns, covering a delay range of $\approx$100 ns from about 5 ns before the laser pulse to 95 ns after the excitation. A representative set of spectral traces at different delay times after the excitation pulse are shown in Fig. 1. From the time-dependent slope of the spectrally integrated PL data shown on a logarithmic scale in the inset of Fig. 1, it is obvious that the temporal evolution cannot be analyzed in terms of a single exponential decay.

As a simple model function for the shape of the PL spectra and their time dependence, we assume a sum of normal-

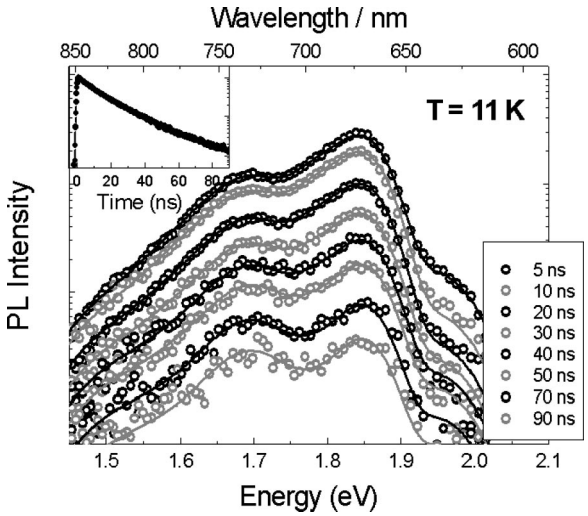

FIG. 1. Evolution of the PTCDA PL spectra as a function of delay after the excitation pulse (circles). The data are shown on a logarithmic scale, and each trace for a given delay t corresponds to a time-integration over an interval of 2.5 ns, i.e., $(t-1.25$ ns,$t+1.25$ ns), for a representative sample of delay times $t=5$, 10, 20, 30, 40, 50, 70, and 90 ns. The solid lines represent the calculated curves based on our model for the time-dependent PL. For clarity, five consecutive spectral data points of the streak camera are summed up, resulting in 96 points with a sampling interval of 2.925 nm. The inset shows the decay of the PL intensity integrated over the whole spectral range on a logarithmic scale.

ized Gaussians with positions ω_j and broadenings σ_j, allowing for time-dependent prefactors $a_j(t)$,

$$I_{PL}(\hbar\omega,t)=\omega^3\sum_{j=1}^{6}\frac{a_j(t)}{\sigma_j\sqrt{2\pi}}\exp\left[-\frac{1}{2}\left(\frac{\omega-\omega_j}{\sigma_j}\right)^2\right], \quad (1)$$

where the multiplicative factor ω^3 is related to the density of states of the emitted photons.[14] In order to define the line shape of the different contributions with a low signal-to-noise ratio, the positions ω_j and the broadenings σ_j were fitted to the time-integrated spectra $I_{PL}(\hbar\omega)=\int dt I_{PL}(\hbar\omega,t)$, so that their weights give the time-integral $A_j=\int dt a_j(t)$ extending over our delay range from small negative delay to 95 ns after the excitation pulse. The results for the time-integrated spectra are reported in Table I and the inset of Fig. 2. In this fitting procedure it turned out that the maximum number of Gaussians resulting in a stable fit was 6, and even in this case, one of the three parameters of the lowest PL band had to be kept fixed, cf. Table I. The narrowest peak at 1.854 eV shows a full width half maximum of about 70 meV, in keeping with the low-temperature absorption linewidth assigned to the low-frequency internal breathing modes and external phonons,[13] while the higher harmonics at lower PL energy have somewhat larger broadenings, as expected from the different internal vibrations contributing.[15] The time-integrated PL spectrum in the inset of Fig. 2 agrees quite well with the so-called Y component of the PL of polycrystalline PTCDA observed earlier.[7] The parameters of two of the PL bands at 1.70 and 1.63 eV are strongly interrelated, so that the uncertainties of their intensities are quite large; cf. Table I. In a fit based on five Gaussians only, the total intensity of the corresponding structure is well defined, resulting however in a significantly larger rms deviations of the measured time-integated PL spectra, so that all six contributions are really required.

TABLE I. Gaussian contributions to the model function [Eq. (1)] for the time-integrated PL spectra, where each of the prefactors A_j can be expressed as an integral $A_j=\int dt a_j(t)$ over the delay-dependent contributions $a_j(t)$. The full widths at half maximum (FWHM's) can be related to the broadening parameters σ in Eq. (1) by a FWHM$_j$ of $\sqrt{8\ln 2}\hbar\sigma_j$. The sum over the time-integrated coefficients A_j is normalized to 100%.

$\hbar\omega_j$ /meV	FWHM$_j$ /meV	A_j /%
1949±5	101±13	2.0±0.3
1853±2	69±3	26.2±8.8
1799±8	92±24	26.4±12.1
1698±5	104±23	26.4±22.3
1631±57	123±37	12.2±19.6
1530 (fixed)	158±10	6.9±0.5

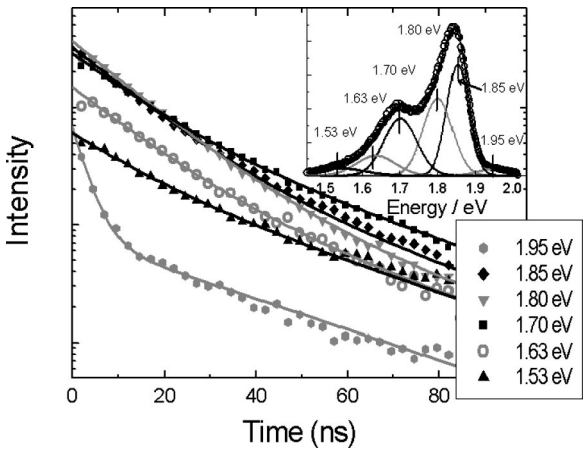

FIG. 2. Time-dependent prefactors of the 6 different contributions to the PL spectra (shown in the inset), and fitting curves based on our bi-exponential decay model (solid lines). The model curve for the PL feature at the highest energy contains components decaying on the fast and slow time scales $\tau_f=3$ ns and $\tau_s=33.5$ ns, respectively, while all other PL bands are based on the two decay times $\tau_m=12.7$ ns and $\tau_s=33.5$ ns, cf. Eqs. (2) and (3).

From the spectrally integrated data in the inset of Fig. 1, we found evidence of a decay with three exponentials: a fast time scale $\tau_f=(3\pm1)$ ns, an intermediate decay time $\tau_m=(12.7\pm0.4)$ ns, and a slow exponential decay with $\tau_s=(33.5\pm2)$ ns. In a second step, we extracted the time-dependent prefactors $a_j(t)$ for different delays t, keeping the position and shape of the six PL bands fixed, cf. Fig. 2. On the logarithmic scale of Fig. 2, the time-dependent slope of the intensities $a_j(t)$ again reveals a nonexponential decay for each of the different contributions to the PL spectra. However, it turns out that the assumption of a biexponential decay for each of the $a_j(t)$'s in the time range $t>4$ ns resulted in a good agreement with the measured data, while the initial dynamics are more complicated, as will be discussed in sub-

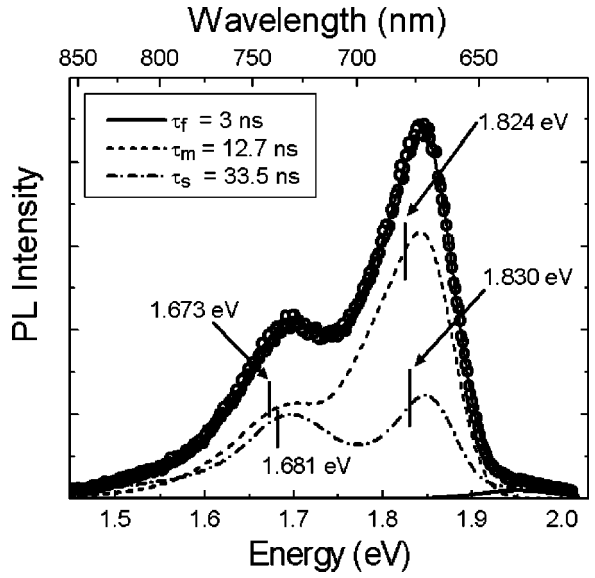

FIG. 3. Time-integrated PL spectrum (circles), together with the contributions of the three different decay channels (fast: solid line, intermediate: dashed line; slow: dash-dotted line).

sequent work. Furthermore, for all PL contributions except for the high-energy feature at 1.95 eV it was possible to model the time traces with the *same* two decay times,

$$a_j(t) = b_j^m e^{-t/\tau_m} + b_j^s e^{-t/\tau_s}, \tag{2}$$

while the highest PL band was the only one containing the fastest decay, with a negligible contribution of the intermediate time scale:

$$a_j(t) = b_j^f e^{-t/\tau_f} + b_j^s e^{-t/\tau_s}. \tag{3}$$

Based on the assumptions made above we can now calculate the PL spectra for different delays (cf. Fig. 1), as all prefactors $a_j(t)$ now have well defined time dependences. From the excellent agreement at all times, we conclude that the temporal evolution of the PL spectra is dominated by the three exponential decay processes included in our model. For each of them we can reconstruct the line shape (cf. Fig. 3), where the fastest component contributes only to the weak high-energy PL band.

The contributions decaying with τ_m and τ_s contain both a vibronic progression with an energy difference of about 0.15 eV, significantly lower than the distance of about 0.17 eV between consecutive vibrational bands in the absorption and PL of dissolved PTCDA (Refs. 1 and 5) as well as the effective internal mode of 0.17 eV used in a recent model calculation of the linear optical properties of PTCDA films.[4] In the latter approach, based on the transfer of Frenkel excitons, it was shown that the exciton dispersion shows a minimum at the surface of the Brillouin zone. After a subtraction of the reorganization energy related to low-frequency internal breathing modes and external phonon modes, the minimum of the exciton dispersion results in a Davydov doublet at 2.038 and 2.043 eV.[13] As these lowest relaxed excited states are indirect in **k** space, they cannot produce PL light without an absorption or emission of a vibronic excitation required for momentum conservation. However, a recombination toward a final state including a vibronic excitation carrying the initial wave vector can result in the emission of a PL photon with $\mathbf{k} \approx \mathbf{0}$.

Based on the same approach as for the calculation of absorption[4] and the dispersion of the Frenkel exciton,[13] it can be shown[16] that both Davydov components result in nearly degenerate PL bands at about 1.83 and 1.68 eV, in good agreement with the peak positions in Fig. 3. Furthermore, the corresponding dipole matrix elements for these PL transitions are much lower than the total highest occupied–lowest unoccupied molecular orbital transition dipole moment of the monomer, resulting in reduced radiative recombination rates, in good agreement with both the decay time and the line shape of the dominating PL contribution in Fig. 3 decaying with $\tau_m = (12.7 \pm 0.4)$ ns.

In the line shape of the slow PL component in Fig. 3, the area of the second harmonics around 1.68 eV corresponds roughly to the area of the first harmonics around 1.83 eV, while the expected relative intensity of the second harmonics resulting from the Poisson progression would be much lower. This is an indication of a further slowly-decaying PL channel around 1.64 eV, corresponding to the charge-transfer PL band becoming more prominent at higher temperature.[17] As can be derived from microscopic calculations for a stack of an anionic and a cationic molecule, this PL channel involves recombination of the excess electron in an anionic molecule towards a positive charged stack neighbor,[13] while the largest subband around 1.83 eV results from a pair of inequivalent molecules in the crystal unit cell with positive and negative charges, respectively.[17,18] The temperature dynamics of the different recombination channels have been discussed elsewhere,[17] including a further PL band around 1.75 eV at higher temperatures[12] arising from a self-trapped exciton.

The high-energy PL feature at 1.95 eV occurs about 90 meV below the minimum of the dispersion of the Frenkel exciton at the surface of the Brillouin zone. As this minimum is indirect, any radiative recombination arising from it still requires the emission of phonons for wave vector conservation. Probably, the additional redshift of about 90 meV is composed of the reorganization energy of about 55 meV related to low-frequency internal breathing modes and external phonons,[13] and the emission of additional vibrational quanta related to these low-frequency modes. Furthermore, the cut-off filter at 2.10 eV could influence the details of the shape of this high-energy PL band. As one of its decay times coincides roughly with the 4 ns assigned to MePTCDI monomers in earlier studies, it could also be related to monomer PL, even though our laser energy of 2.14 eV is not sufficient for the expected transition energy E_{00} between the lowest vibronic levels. Alternatively, this fastest decay rate could also involve nonradiative recombination processes. In any case, from the smallness of this PL band, it is obvious that the corresponding recombination processes are less efficient than for the other PL contributions.

As a conclusion, within a time window of about 100 ns, we have found two slow decay times in time-resolved PL spectra of crystalline PTCDA, both much slower than

previously reported for Me-PTCDI and PTCDA thin films.[6,11,12] The recombination channel decaying on the intermediate time scale $\tau_m = 12.7 \pm 0.4$ ns is assigned to the Frenkel exciton PL starting from the minimum of the exciton dispersion at the surface of the Brillouin zone, while the slowest PL channel is assigned to the recombination between positively and negatively charged molecules.

ACKNOWLEDGMENTS

The authors gratefully acknowledge the DFG-funded Graduiertenkolleg ''Dünne Schichten und nichtkristalline Materialien'' at the Technical University of Chemnitz, and the EU funded Human Potential Research Training Network DIODE (Contract No. HPRN-CT-1999-00164) for financial support.

[1] S. R. Forrest, Chem. Rev. **97**, 1793 (1997).
[2] A. Djurišić, T. Fritz, and K. Leo, Opt. Commun. **183**, 123 (2000).
[3] M. I. Alonso, M. Garriga, N. Karl, J. O. Ossó, and F. Schreiber, Org. Electron. **3**, 23 (2002).
[4] I. Vragović, R. Scholz, and M. Schreiber, Europhys. Lett. **57**, 288 (2002).
[5] U. Gómez, M. Leonhardt, H. Port, and H. C. Wolf, Chem. Phys. Lett. **268**, 1 (1997).
[6] F. F. So and S. R. Forrest, Phys. Rev. Lett. **66**, 2649 (1991).
[7] M. Leonhardt, O. Mager, and H. Port, Chem. Phys. Lett. **313**, 24 (1999).
[8] K. Puech, H. Fröb, M. Hoffmann, and K. Leo, Opt. Lett. **21**, 1606 (1996); K. Puech, H. Fröb, and K. Leo, J. Lumin. **72-74**, 524 (1997).
[9] H. Nishimura, T. Yamaoka, K. Mizuno, M. Iemura, and A. Matsui, J. Phys. Soc. Jpn. **53**, 3999 (1984).
[10] M. Hoffmann, K. Schmidt, T. Fritz, T. Hasche, V. M. Agranovich, and K. Leo, Chem. Phys. **258**, 73 (2000).
[11] A. Nollau, M. Hoffman, T. Fritz, and K. Leo, Thin Solid Films **368**, 130 (2000).
[12] A. Yu. Kobitski, G. Salvan, H. P. Wagner, and D. R. T. Zahn, Appl. Surf. Sci. **179**, 209 (2001).
[13] R. Scholz, I. Vragović, A. Yu. Kobitski, G. Salvan, T. U. Kampen, M. Schreiber, and D. R. T. Zahn, in *Proceedings of the International School of Physics ''E. Fermi,'' Course CXLIX: Organic Nanostructures: Science and Applications* (IOS Press, Amsterdam, 2002).
[14] R. Loudon, *The Quantum Theory of Light* (Clarendon, Oxford, 1983), Chap. 2.4.
[15] R. Scholz, A. Yu. Kobitski, T. U. Kampen, M. Schreiber, D. R. T. Zahn, G. Jungnickel, M. Elstner, M. Sternberg, and T. Frauenheim, Phys. Rev. B **61**, 13659 (2000).
[16] R. Scholz, I. Vragović, A. Yu. Kobitski, M. Schreiber, H. P. Wagner, and D. R. T. Zahn, Phys. Status Solidi B (to be published).
[17] R. Scholz, A. Yu. Kobitski, I. Vragović, T. U. Kampen, H. P. Wagner and D. R. T. Zahn, in *Proceedings of the 26th International Conference on the Physics of Semiconductors* (IOP, Bath, 2002).
[18] R. Scholz, A. Yu. Kobitski, and D. R. T. Zahn (unpublished).